COMMUNICATIONS IN NUMERICAL METHODS IN ENGINEERING
Commun. Numer. Meth. Engng 2000; **00**:1–12 *Prepared using* cnmauth.cls *[Version: 2000/03/22 v1.0]*

A FULLY COUPLED NUMERICAL MODEL FOR TWO-PHASE FLOW WITH CONTAMINANT TRANSPORT AND BIODEGRADATION KINETICS

CLAUDIO GALLO[1] AND GIANMARCO MANZINI[2]*

[1] *CRS4, Zona Industriale Macchiareddu, Uta, Cagliari - Italy*
[2] *IAN - CNR, via Ferrata 1, 27100 Pavia, Italy*

SUMMARY

A fully coupled numerical model is presented which describes biodegradation kinetics and NAPL-aqueous two-phase flow in porous media. The set of governing partial differential equations is split in two sub systems, the former one in terms of phase pressure and saturations, and the latter one in terms of contaminant concentration and bacterial population distribution. Non-linear saturation dependence in Brooks-Corey relative permeability functions and capillary pressure effects are incorporated in a mixed-hybrid finite element model. The non-linear degradation kinetics *à la* Monod is taken into account as a source term in the finite volume discretization of the equation modeling contaminant transport. The global coupling is performed by using a nested block-iteration technique. A set of numerical experiments demonstrates the effectiveness of the method. Sensitivity analysis results are also presented. Copyright © 2000 John Wiley & Sons, Ltd.

KEY WORDS: bioremediation, Two-phase flow, mixed finite elements, finite volumes

1. INTRODUCTION

An organic contaminant leaking in groundwater is generally advected as a separate *non-aqueous phase liquid* (NAPL) one, but may also be partially dissolved in the *aqueous phase*, namely water. This dissolved part of NAPL is liable to be degraded by the bacterial population naturally present in soil. A major simplification in the mathematical and numerical modelling of such a process accounts for the contaminant as a solute passively transported in the aqueous phase [2, 8, 9], no taking care of the presence of different phases. However, a better understanding of the underlying phenomena needs an explicit description in terms of a multi-phase flow model coupled with a transport equation for the contaminant dissolved in water [6, 7]. The dissolved NAPL contaminant is degraded according with a Monod-type kinetics, see for instance Reference [11].

It is worth mentioning that transport of contaminants may often take place in rather deformable porous media. Hence, the multi-phase flow model should also be completed by

*Correspondence to: Gianmarco Manzini, IAN - CNR, via Ferrata 1, 27100 Pavia, Italy

Received : XXX
Revised : XXX
Accepted : XXX

including soil displacement effects, as in References [10, 12, 13]. In this work we explore a numerical coupling of contaminant transport and biodegradation in the framework of a simple two-phase flow model and its preliminary application to 1-D sensitivity analysis. Extension to more complex scenarios, which may deserve for special numerical treatments, will be the subject of future work. The discretization relies on a block-iterative splitting algorithm, and separates the mathematical model in two sets of equations, the former for phase pressures and saturations and the latter for contaminant transport and biodegradation. Pressure/saturation equations are re-formulated in terms of total pressure and velocity fields following the approach of Chavent and Jaffré, see Reference [5]. The main reason for this approach is that efficient numerical methods can be devised to take advantage of the physical properties inherent in the flow equations. This set of equations is approximated by the discontinuous lowest order mixed-hybrid Raviart-Thomas finite element method [3]. The saturation equations are then approximated by cell-center finite volumes and advanced in time by an explicit two-stage Runge-Kutta scheme. In the second set of equations, a predictor-corrector strategy decouples the advective transport of the dissolved contaminant concentration from the source reaction term which describes the consumption by soil bacterial population. The differential equation that modellizes growth and decay of bacteria is analytically solved at any iterative step of the computation after updating the dissolved contaminant concentration field [9]. The outline of the paper is the following. In section 2 we introduce the mathematical model, in section 3 we focus on the iterative splitting approach and shortly discuss the numerical techniques, and in section 4 we present some preliminary 1-D numerical results.

2. MATHEMATICAL MODEL

The two-phase flow is governed by the couple of phase conservation equations

$$\frac{\partial}{\partial t}(\phi\rho_l s_l) + \nabla\cdot\mathbf{F}_l = q_l + q_{ln}\,, \tag{1}$$

$$\frac{\partial}{\partial t}(\phi\rho_n s_n) + \nabla\cdot\mathbf{F}_n = q_n - q_{ln}\,, \tag{2}$$

where the subscripts l and n refer to aqueous and non-aqueous phases, t is the time, ϕ is the porosity, ρ_l and ρ_n are the constant phase densities, s_l and s_n are the saturations, q_l and q_n are the mass source/sink terms, q_{ln} is a mass exchange term between the two phases. The advective fluxes $\mathbf{F}_l$ and $\mathbf{F}_n$ take the usual Darcy's form

$$\mathbf{F}_l = -\rho_l\lambda_l\mathbf{K}\cdot\nabla(P_l + \rho_l g h) = \rho_l\mathbf{v}_l\,, \tag{3}$$

$$\mathbf{F}_n = -\rho_n\lambda_n\mathbf{K}\cdot\nabla(P_n + \rho_n g h) = \rho_n\mathbf{v}_n\,, \tag{4}$$

where P_l and P_n are the pressure fields, $\mathbf{K}$ is the absolute permeability tensor, λ_l and λ_n are the phase mobilities, $\mathbf{v}_l$ and $\mathbf{v}_n$ are the phase velocities, g is the gravitational constant and h is the head above a given datum. Phase mobilities are defined as

$$\lambda_l = \frac{k_{rel,l}}{\mu_l}\,, \qquad \lambda_n = \frac{k_{rel,n}}{\mu_n}\,, \tag{5}$$

where $k_{rel,l}$ and $k_{rel,n}$ are the soil relative permeabilities, μ_l and μ_n are the viscosities.

Let us assume that densities and viscosities are constant (isothermal system assumption), and that, as usual, saturations sum to unity. Following the ideas of Chavent [5], we can re-state (1-2) in terms of the aqueous phase pressure P_l and the total velocity $\mathbf{v}_T = \mathbf{v}_l + \mathbf{v}_n$ which satisfy

$$\begin{cases} \nabla \cdot \mathbf{v}_T &= Q_T\,, \\ \mathbf{v}_T &= -(\lambda_l + \lambda_n)\,\mathbf{K} \cdot \nabla P_l + \mathbf{Q}_S\,. \end{cases} \tag{6}$$

The global source terms $\mathbf{Q}_S$ and Q_T are given by

$$\mathbf{Q}_S = \mathbf{K} \cdot \mathbf{q}_S\,, \quad Q_T = \frac{q_l}{\rho_l} + \frac{q_n}{\rho_n}\,, \tag{7}$$

with

$$\mathbf{q}_S = -\left(\lambda_l \rho_l + \lambda_n \rho_n\right) \mathbf{g} - \lambda_n P_c' \nabla s_l\,, \tag{8}$$

where $\mathbf{g} = \nabla(g\,h)$ is the gravity vector. Assuming water as the wetting fluid, we introduced in (8) the capillary pressure defined as $P_c = P_n - P_l$.

Phase velocities are then given back by

$$\mathbf{v}_l = \frac{\lambda_l}{\lambda_l + \lambda_n}(\mathbf{v}_T - \mathbf{Q}_S) - \lambda_l \rho_l \mathbf{K} \cdot \mathbf{g}\,, \tag{9}$$

$$\mathbf{v}_n = \mathbf{v}_T - \mathbf{v}_l. \tag{10}$$

The transport of the dissolved NAPL contaminant concentration C by the water bulk motion is described by

$$\frac{\partial(\phi s_l C)}{\partial t} + \nabla \cdot (\mathbf{v}_l C) = q_{ln} - q_{bio}\,. \tag{11}$$

The source term q_{ln} takes into account the mass transfer process from NAPL to aqueous phase. This term is linearly proportional to the difference between the maximum concentration of NAPL that can be dissolved in water at equilibrium, C^{eq}, and its actual concentration, C, i.e.

$$q_{ln} = \phi s_n k_{do}(C^{eq} - C)\,. \tag{12}$$

The mass transfer proportionality coefficient is denoted by k_{do}.

The sink term q_{bio} is responsible for biodegradation and takes the form

$$q_{bio} = N_c m_c Y \mu_{bio} \left[\frac{C}{K_{1/2} + C}\right]\,, \tag{13}$$

where μ_{bio} is the maximum degradation rate, $K_{1/2}$ the half-saturation constant, N_c the number of bacterial colonies per unit volume, m_c the mass of a colony, and Y a yield coefficient [11].

Finally, the rate of microbial growth/decay is obtained by balancing bio-mass reproduction and decay

$$\frac{1}{N_c}\frac{\partial N_c}{\partial t} = \left(\mu_{bio}\left[\frac{C}{K_{1/2} + C}\right] - k_d\right) \tag{14}$$

where the parameter k_d is the bacterial decay constant [8,11].

Finally, some constitutive relations must be specified to get closure of the model. Saturations depend on P_c via the Brooks-Corey relation [4],

$$P_c = P_d * s_{le}^{-1/\lambda}\,. \tag{15}$$

In equation (15), P_d is the entry pressure, λ a fitting parameter related to the pore-size distribution, s_{le} the effective liquid saturation, defined as $s_{le} = (s_l - s_{lr})/(1 - s_{lr} - s_{nr})$, and s_{lr} and s_{nr}, respectively, the wetting- and nonwetting-phase residual saturations. The relative permeabilities are given by

$$k_{rel,l} = (s_{le})^{\alpha}\,, \qquad k_{rel,n} = (1 - s_{le})^{\alpha}\,, \tag{16}$$

the value of the parameter α being fitted via regression on experimental data.

3. NUMERICAL MODEL

Basically, our discretization approach consists in an external loop in time, namely `[Global]`, split in two internal loops, namely `[P-S]` and `[C-bio]`. The loop `[P-S]` updates the phase pressures P_l and P_n and the saturations s_l and s_n, by solving iteratively system (6) and equations (1-2). The loop `[C-bio]` updates the concentration of the NAPL contaminant dissolved in water and the microbial population distribution.

At any time step, the outer loop alternatively iterates on the two inner loops until convergence is reached:

while $t < t_{max}$

  loop `[Global]` **until** convergence

    loop `[P-S]` **until** convergence
    loop `[C-bio]` **until** convergence
    check global convergence

  end loop
  $t = t + \Delta t$

end while

The loop `[P-S]` takes the form

loop `[P-S]` **until** convergence

  estimate $\nabla S^{t+\Delta t,k}$ **from** $S^{t+\Delta t,k}$
  solve for $P_l^{t+\Delta t,k+1}$ **and** $\mathbf{v}_T^{t+\Delta t,k+1}$ [system (6)]
  estimate $\mathbf{v}_l^{t+\Delta t,k+1}$ **and** $\mathbf{v}_n^{t+\Delta t,k+1}$ **by using** $S^{t+\Delta t,k}$ [equations (9-10)]
  solve for $S^{t+\Delta t,k+1}$ [equations (1-2)]
  check $||S^{t+\Delta t,k+1} - S^{t+\Delta t,k}|| \le \epsilon_{[P-S]}$

end loop

where S denotes the vector of unknowns $(s_l,\, s_n)^T$, k is the iteration index, $\epsilon_{[P-S]}$ is a user-specified tolerance, and $||\cdot||$ is the Euclidean norm.

At each internal step, system (6) is solved by approximating the normal component of the total velocity field at cell interfaces, $\mathbf{v}_T \cdot \mathbf{n}$ say, by the discontinuous lowest order mixed-hybrid Raviart-Thomas finite elements and the aqueous phase pressure P_l by piecewise constant elements over the computational cells and at cell interfaces [3]. Let us denote these approximate fields by respectively $\mathbf{q}_h$, ψ_h and λ_h. The symbol h denotes the maximum diameter of all the cells K in a given mesh $\mathcal{T}_h$, $|K|$ is the cell volume and ∂K the cell boundary. The variational formulation reads as

$$\begin{cases} \displaystyle\int_\Omega \frac{\mathbf{K}^{-1}}{(\lambda_l+\lambda_n)}\mathbf{q}_h\cdot\mathbf{w}_h - \sum_K \int_K \psi_h \nabla\cdot\mathbf{w}_h + \sum_K \int_{\partial K} \lambda_h\,\mathbf{w}_h\cdot\mathbf{n}_K = \int_\Omega \mathbf{Q}_S\cdot\mathbf{w}_h\,, \\ \displaystyle\sum_K \int_K v_h \nabla\cdot\mathbf{q}_h = \int_\Omega Q_T v_h\,, \\ \displaystyle\sum_K \int_{\partial K} \mathbf{q}_h\cdot\mathbf{n}_K \mu_h = 0\,, \end{cases} \tag{17}$$

where the test functions $\mathbf{w}_h$, v_h and μ_h are taken in the same functional spaces of the corresponding unknowns. Standard algebraic manipulations yields a linear problem which is solved for the set of Lagrangian multipliers λ_h by using the static condensation technique. Backward substitution closes the solution algorithm [3]. This non-conforming finite element method guarantees that a zero-divergence constraint is well satisfied by the total velocity field. This issue is required to fairly simulate the non-linear degradation kinetics, as pointed out in [7].

The semi-discrete finite volume formulation that approximates equations (1-2) is obtained by integrating separately in a cell-wise fashion each phase saturation equation, applying the divergence theorem, approximating the interface integrals with the midpoint rule, and finally computing the advective fluxes by an upwind estimation of the phase velocities $\mathbf{v}_l$ and $\mathbf{v}_n$. This method takes the form

$$\begin{aligned} |K|\frac{dS_K}{dt} &+ \sum_{k\in\sigma(K)} l_k H(S_k^{int}, S_k^{ext}, \mathbf{n}_k) + \\ &\sum_{k'\in\sigma'(K)} l_{k'} H_{k'}^{(bc)}(S_k^{int}) = |K|Q(S_K), \qquad \forall K\in\mathcal{T}_h, \end{aligned} \tag{18}$$

where S_K indicates the K-th cell-averaged value for both s_l and s_n, $\sigma(K)$ is the set of cells adjacent to K, $\sigma'(K)$ is the set of boundary edges on ∂K, $H(S_k^{int}, S_k^{ext}, \mathbf{n}_k)$ and $H_{k'}^{(bc)}(S_k^{int})$ are the numerical fluxes at internal and boundary edges, $Q(S_K)$ stands for the source terms in (1-2), and l_k, $l_{k'}$ are the edge lengths. The numerical fluxes depend on S_k^{int} and S_k^{ext}, which are the traces at each cell interface of the linearly reconstructed saturation. The boundary flux $H_{k'}^{(bc)}(S_k^{int})$ may also depend on a set of suitable *external* data. A special linear reconstruction procedure interpolates the cell-averaged saturation values $\{S_K\}_{K\in\mathcal{T}_h}$ and ensures a TVD stability condition by limiting the reconstructed slopes. This avoids order one oscillations to appear in sharp gradient solution regions [7]. An explicit two-stage 2^{nd}-order Runge-Kutta scheme advances in time the approximate solutions S_K. The method is formally second order accurate [9].

A predictor-corrector strategy is deserved to treat the non-linear dependence on C in the sink source term q_{bio}

loop `[C-bio]` **until** convergence

> **compute** $\tilde{C}^{t+\Delta t,m+1}$ [equation (11) with $q_{bio}=0$]
> **estimate** q_{ln} **by using** $\tilde{C}^{t+\Delta t,m+1}$ [equation (13)]

compute $C^{t+\Delta t,m+1}$ **by using** $\tilde{C}^{t+\Delta t,m+1}$ **and** q_{bio} [equation (11)]
compute $N^{t+\Delta t,m+1}$ [equation (14)]
check: $||C^{t+\Delta t,m+1} - C^{t+\Delta t,m}|| \leq \epsilon_{[C-bio]}$

end loop

where $\epsilon_{[C-bio]}$ is a user-defined tolerance. The field $\tilde{C}^{t+\Delta t,m+1}$ is initially predicted by assuming $q_{bio} = 0$ in (11). Then, the bacterial consumption source term is evaluated by using $\tilde{C}^{t+\Delta t,m+1}$ in equation (13). Finally, equation (11) is re-iterated with the estimated value of q_{bio} to correct the dissolved contaminant concentration field at $t + \Delta t$. The new bacterial population is calculated using this latter concentration value in equation (14). The whole procedure is iterated until convergence. As for the phase saturations, the concentration equation is discretized by using a second order finite volume scheme. Further details are given in Reference [9].

4. NUMERICAL EXPERIMENTS

4.1. Validation

The different parts of the numerical simulator were separately validated on a set of suitable model problems. The validation of the contaminant transport solver and the biodegradation module are part of a previous work, see Reference [9], and will not be discussed herein.

The coupled two-phase flow solver in loop `[P-S]` has been extensively validated by comparing numerical results with the exact solution of the classical 1-D Buckley-Leverett problem in a set of representative situations [1], an example of whose is given in Figure 1. This calculation was performed using 40 cells, and a good agreement is evident between the exact and the numerical solution. The combined rarefaction wave-shock discontinuity pattern is due to the non-convexity of the physical flux function and is captured quite fairly. Discontinuities are approximated in at worst four cells and little dissipative smearings characterize rarefaction waves.

4.2. 1-D column simulations

At $t = 0$ a ten meter length homogeneous porous medium column is completely filled in the range [0, 200 cm] by a NAPL contaminant with constant saturation $s_N = 0.16$. The water phase saturation in the rest of the column is $s_L = 1.0$. The bacterial population is uniformly distributed. At $t > 0$ the column is flushed by pure water and the NAPL contaminant begins to dissolve and be degraded. The computational domain is discretized by using 250 1-D regular cells and a time-step $\Delta t = 1$ sec. The value of the mass-transfer coefficient k_{do} ranges throughout 10^{-7} and 10^{-4} s^{-1}, while the maximum degradation rate, μ_{bio}, ranges throughout $3.4 * 10^{-8}$ and $3.4 * 10^{-4}$ s^{-1}. The values of the other parameters in the simulations are given in Table I.

The column distributions of the water saturation s_l at different instants of the simulation are shown with and without biodegradation in Figure 2. The condition $s_n = s_{nr}$ is earlier verified when biodegradation takes place, thus implying that NAPL trapping effects, namely immobilization, are enhanced.

Table I. Values of the parameters in 1-D column simulations.

ϕ	ρ_n (Kg/m^{-3})	$\|\mathbf{K}\|$ (m^2)	k_d (s^{-1})	C^{eq} (g/l)	$K_{1/2}$ (g/l)
0.74	1.000	10^{-8}	$2.14 * 10^{-7}$	0.02	0.02

Table II. Performance of the non-linear iterative procedure

k_{do} (s^{-1})	$N_G^{\Delta t}$	$N_{PS}^{\Delta t}$	$N_{Cbio}^{\Delta t}$	N_{PS}^{G}	N_{Cbio}^{G}
10^{-4}	2.9	15.1	8.6	5.2	2.9
10^{-5}	2.0	8.4	5.0	4.3	2.5
10^{-6}	2.0	8.4	5.0	4.2	2.5
10^{-7}	1.8	8.4	4.8	4.2	2.4

4.2.1. Convergence of the non-linear iterative scheme. Table II illustrates the effectiveness of the split iterative scheme described in the previous section. We evaluate the performance of the method by measuring the iterations required to get convergence in both internal loops and in the external one.

From the left-most to the right-most column of the table, k_{do}, is the mass-transfer coefficient; $N_G^{\Delta t}$, $N_{PS}^{\Delta t}$, and $N_{Cbio}^{\Delta t}$ are the average number of iterations per time step required to achieve convergence in respectively the outer loop `[Global]` and the inner loops `[P-S]` and `[C-bio]`; N_{PS}^{G} and N_{Cbio}^{G} are the average number of iterations per global iteration to achieve convergence in the inner loops.

The performance table illustrates that convergence is achieved in `[P-S]` and `[C-bio]` in a comparable number of iterations, even if the former loop demands for about three-half the number of iterations of the latter one. Decreasing the value of k_{do} below 10^{-4} s^{-1}, the computational effort needed to solve the two inner loops does not change significantly, and attains reasonable values, that is the average number of inner iterations per global one is always between `2.5` and `5.5`.

4.2.2. Sensitivity analysis. Cumulative effects are analyzed in the transient $[0,T]$ by considering the mass fraction of the NAPL contaminant dissolved in water

$$M^*_{diss}(T) = \frac{M_{diss}}{M_{tot,t=0}} = \frac{\displaystyle\int_0^T \int_L \phi s_n q_{ln}\, dx dt}{\displaystyle\int_L \phi s_n|_{t=0} \rho_n\, dx}, \tag{19}$$

and the one degraded by bacteria

$$M^*_{deg}(T) = \frac{M_{deg}}{M_{tot,t=0}} = \frac{\displaystyle\int_0^T \int_L \phi s_l q_{bio} dx dt}{\displaystyle\int_L \phi s_n|_{t=0} \rho_n\, dx}. \tag{20}$$

The two adimensional groups

$$\begin{aligned} V &= (|\mathbf{K}|\Delta P_{max})/(\mu_l k_{do} L^2), \\ R &= (N_{c,0} m_c \mu_{bio})/(\rho_l k_{do}), \end{aligned} \tag{21}$$

have been recognized and used as independent parameters in our numerical sensitivity analysis.

We stress that both parameters, as defined in (21), may be given a physical interpretation. In fact, V is a sort of inverse ratio of the characteristic time of the flow to the characteristic time of the mass-transfer process, while R of the inverse ratio of the characteristic time of degradation kinetics to the characteristic time of the mass-transfer process.

In equations (20) and (21) ΔP_{max} is the pressure gradient between the two ends of the column, L is the column length, and $N_{c,0}$ is the average initial concentration of bacteria. Figure 3 shows the dependence on V and R of M^*_{diss} and M^*_{deg}. Three distinct regimes can be identified from left to right: a mass-transfer limited one, a transition one, and a kinetics-limited one. For the lowest values of V, i.e. the left-most parametric curves in Figure 3, a little variation of the smallest value of R may produce significant changes in the total dissolved and degraded mass. Instead, the system behavior is less dependent on the choice of R for increasing values of V, that is the dissolved mass tends to stabilize to a constant value. It is informative to say that all the values of R were obtained by using the same value of μ_{bio}, except in the case of the minimum value of V. This latter situation is the one more strongly influenced by a variation in R. In facts, when small values of μ_{bio} occurs, the contaminant concentration gradient, which is roughly proportional to $(C^{eq} - C)$, is very small. Thus, equilibrium conditions are nearly attained, and we may expect that the NAPL contaminant be very poorly degraded. Since in this case the dissolution process is likely to be almost depressed, only incoming pure water can buffer the dissolved NAPL contaminant and only a variation in the flow condition can modify the dissolution rate.

5. CONCLUSION

A numerical model was investigated which couples phase pressure and saturations in two-phase flow and NAPL concentration transport and biodegradation kinetics. A mixed-hybrid finite element model incorporates the non-linear saturation dependence in Brooks-Corey relative permeabilities and capillary pressure effects. A finite volume method takes into account the contaminant concentration transport which also incorporates the non-linear degradation kinetics as a suitable source term. One-dimensional numerical simulations were performed for a homogeneous porous medium and illustrate the effectiveness of the approach in predicting significant effects in the behavior of the contaminant distribution. The approach addressed in the paper has satisfactorily been tested against a set of relevant situations in 1-D column flow simulations.

ACKNOWLEDGEMENTS

Part of this work was performed by the first author (C. G.) at the Faculty of Civil Engineering and Geosciences in Delft, The Netherlands, whose hospitality and financial support are gratefully acknowledged.

The work was also supported by the Italian C.N.R. and the Sardinian Regional Authorities.

The authors appreciated the constructive criticism of the anonymous reviewers, whose many suggestions were helpful in improving the paper.

REFERENCES

1. M. B. Allen III, A. Behie, and J. A. Trangenstein. *Multiphase Flow in Porous Media: Mechanics, Mathematics and Numerics.* Lecture Notes in Engineering – Springer-Verlag, 1988.
2. M. Blunt, M. J. King, and H. Scher. Simulation and theory of two-phase flow in porous media. *Physical Review*, 46(12):7680–7699, 1992a.
3. F. Brezzi and M. Fortin. *Mixed and Hybrid Finite Element Methods.* Springer-Verlag, Berlin, 1991.
4. R. H. Brooks and A. T. Corey. Hydraulic properties of porous media. Technical Report Hydrology-3, Colorado State University, Fort Collins, Colorado, 1964.
5. G. Chavent. *A new formulation of diphasic incompressible flows in porous media*, volume 503 of *Lecture Notes in Mathematics.* Springer-Verlag, 1976.
6. R. E. Ewing. The need for multidisciplinary involvement in groundwater contaminant simulations. In G. Delic and M. Wheeler, editors, *Proceedings of Next Generation Environmental Models and Computational Methods, SIAM Conference*, 1997.
7. R. E. Ewing and S. Weekes. Numerical methods for contaminant transport in porous media. *Computational Mathematics*, 202:75–95, 1998.
8. C. Gallo and G. Manzini. 2-D Numerical modeling of bioremediation in heterogeneous saturated soils. *Transport in Porous Media*, 31:67–88, 1998.
9. C. Gallo and G. Manzini. A mixed finite element/finite volume approach for solving biodegradation transport in groundwater. *International Journal of Numerical Methods in Fluids*, 26:533–556, 1998.
10. R. W. Lewis, B. A. Schrefler, and N. Ab. Rahman. A new model for predicting the hydraulic conductivity of porous media. *Comm. Num. Meth. Engrg.*, 14(2):513–522, 1998.
11. F. J. Molz, M. A. Widdowson, and L. D. Benefield. Simulation of microbial growth dynamics coupled to nutrient and oxygen transport in porous media. *Water Resources Research*, 22(8):1207–1216, 1986.
12. N. Ab. Rahman and R. W. Lewis. Finite element modelling of multiphase immiscible flow in deforming porous media for subsurface systems. *Computers and Geotechnics*, 24(1):41–63, 1999.
13. B. A. Schrefler, L. D'Alpaos, X. Y. Zhan., and L. Simoni. Pollutant transport in deforming media - plenary lecture, 2^{nd} european solid mech. conf. *Eur. J. of Mech. A/Solids*, 13(4-suppl.):175–194, 1998.

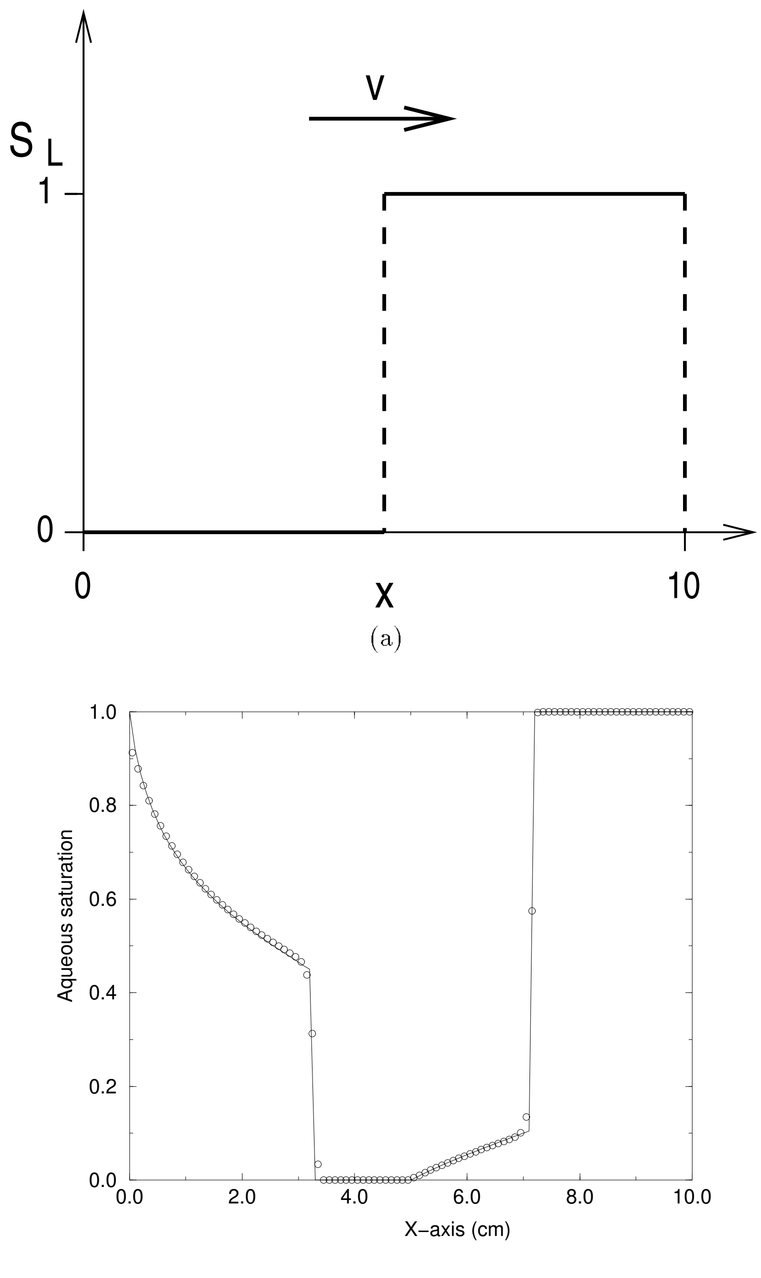

Figure 1. Two-phase flow without bioremediation: (a) the initial solution of the aqueous saturation, (b) the exact solution (solid) and its numerical approximation (circles) at $t = 1$ day.

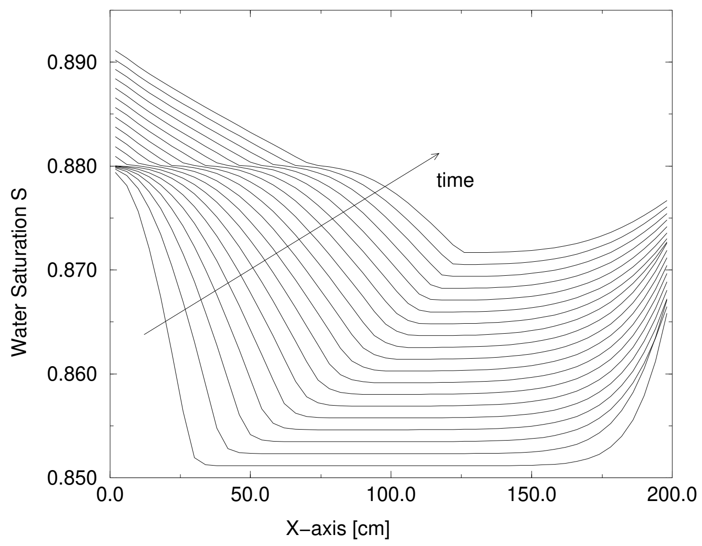

(a)

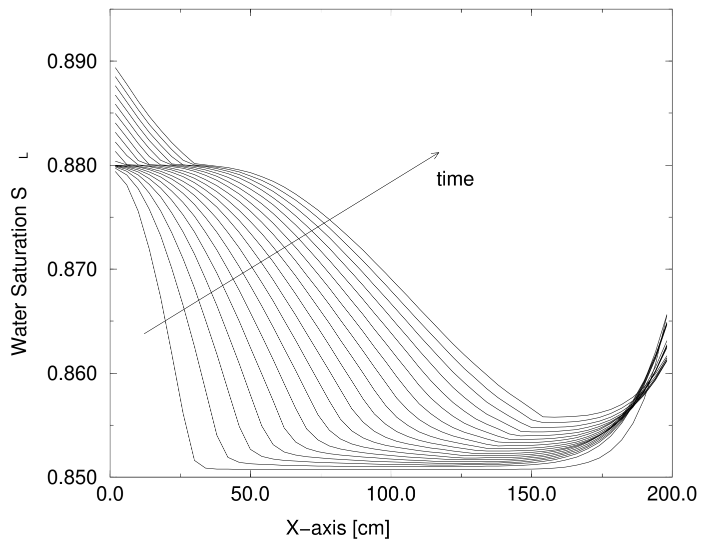

(b)

Figure 2. Aqueous saturation at different times (one curve every 0.5 days): (a) with and (b) without biodegradation. The arrow indicates the direction of increasing time.

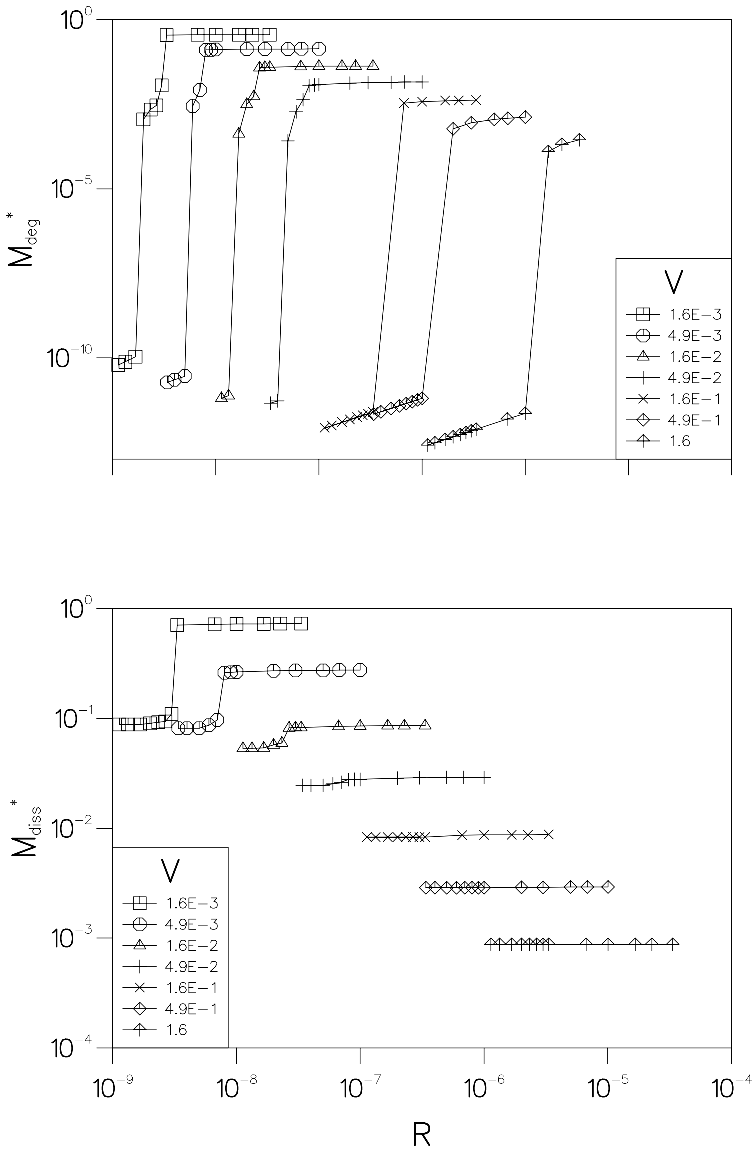

Figure 3. Sensitivity analysis: degraded mass curves, $M^*_{deg}(T)$, and total dissolved mass curves, $M^*_{diss}(T)$, versus the adimensional group R for different values of V.